J Biomol NMR (2012) 53:293–301
DOI 10.1007/s10858-012-9639-0

ARTICLE

Speeding up sequence specific assignment of IDPs

Wolfgang Bermel · Ivano Bertini · Isabella C. Felli · Leonardo Gonnelli · Wiktor Koźmiński · Alessandro Piai · Roberta Pierattelli · Jan Stanek

Received: 8 April 2012 / Accepted: 22 May 2012 / Published online: 10 June 2012

Abstract The characterization of intrinsically disordered proteins (IDPs) by NMR spectroscopy is made difficult by the extensive spectral overlaps. To overcome the intrinsic low-resolution of the spectra the introduction of high-dimensionality experiments is essential. We present here a set of high-resolution experiments based on direct ^{13}C-detection which proved useful in the assignment of α-synuclein, a paradigmatic IDP. In particular, we describe the implementation of 4D HCBCACON, HCCCON, HCBCANCO, 4/5D HNCACON and HNCANCO and 3/4D HCANCACO experiments, specifically tailored for spin system identification and backbone resonances sequential assignment. The use of non-uniform-sampling in the indirect dimension and of the H-flip approach to achieve longitudinal relaxation enhancement rendered the experiments very practical.

Keywords Intrinsically disordered proteins · ^{13}C detection · Non-uniform sampling · Multidimensional NMR experiment · Backbone assignment · Spin system identification

Electronic supplementary material The online version of this article (doi:10.1007/s10858-012-9639-0) contains supplementary material, which is available to authorized users.

W. Bermel
Bruker BioSpin GmbH, Silberstreifen, 76287 Rheinstetten, Germany

I. Bertini (✉) · I. C. Felli · L. Gonnelli · A. Piai · R. Pierattelli
CERM, University of Florence, Via Luigi Sacconi 6, 50019 Sesto Fiorentino, Florence, Italy
e-mail: ivanobertini@cerm.unifi.it

I. Bertini · I. C. Felli · R. Pierattelli
Department of Chemistry "Ugo Schiff", University of Florence, 50019 Sesto Fiorentino, Italy

W. Koźmiński · J. Stanek
Faculty of Chemistry, University of Warsaw, Pasteura 1, 02093 Warsaw, Poland

Introduction

The importance of local flexibility and conformational freedom for protein function is attracting the attention of the scientific community, thanks to many examples of intrinsically disordered proteins (IDPs) or intrinsically disordered regions (IDRs) of modular proteins appearing in the literature. The commonly accepted structure/function paradigm, supported by a vast amount of protein 3D structures deposited in the Protein Data Bank (www.pdb.org), should thus be expanded to take into account that a large share of proteins exist and function without a well-defined folded structure and, actually, in many cases they are able to carry out essential functions thanks to the structural disorder (Wright and Dyson 1999; Uversky et al. 2000; Dunker et al. 2001; Tompa 2002; Dyson and Wright 2005; Tompa 2009). Thanks to the ability to provide atomic resolution information also for very flexible protein fragments, nuclear magnetic resonance (NMR) spectroscopy becomes a strategic tool of investigation (Dyson and Wright 2004; Mittag and Forman-Kay 2007; Eliezer 2009). However, the lack of a stable 3D molecular structure entails a dramatic decrease of the chemical shift dispersion of the NMR signals as the contributions to chemical shifts deriving from the local protein environment are largely averaged out (Zhang et al. 2003; Mittag and Forman-Kay 2007; Kjaergaard and Poulsen 2011; Kjaergaard et al. 2011). Furthermore, the efficient solvent exchange processes for amide protons that in the absence of a stable 3D structure are largely solvent exposed,

may cause broadening of the signals beyond detectable limits (Hsu et al. 2009). Indeed, many studies of IDPs are performed at low temperature and low pH to improve the detection of amide proton signals. To overcome these drawbacks and be able to expand the size and complexity of IDPs/IDRs that can be characterized at atomic resolution it is thus crucial to exploit at best the nuclear spin properties in the design of NMR experiments. Recent improvements in instrumental technology, in conjunction with the growing interest in the study of intrinsically disordered protein states, are stimulating rapid progress in the design of NMR experimental methods. The increased instrumental sensitivity leads to the development of experimental approaches to reduce the duration of NMR experiments (Schanda et al. 2006; Atreya and Szyperski 2005; Hiller et al. 2005; Jaravine et al. 2008; Malmodin and Billeter 2005; Lescop et al. 2007) and/or to exploit direct detection of nuclear spins other than ^{1}H (Serber et al. 2000; Bermel et al. 2003, 2006b; Shimba et al. 2005; Hu et al. 2007). Indeed, a number of exclusively heteronuclear NMR experiments based on ^{13}C direct detection, which take maximum advantage of the improved chemical shift dispersion of heteronuclei and of their reduced susceptibility to exchange broadening, has been developed (Bermel et al. 2006c, 2009, 2010; Bertini et al. 2011b) and proved useful in the characterization of several IDPs (Pasat et al. 2008; Csizmok et al. 2008; Pérez et al. 2009; O'Hare et al. 2009; Knoblich et al. 2009). Elegant approaches exploiting longitudinal relaxation rate enhancement (LRE) (Pervushin et al. 2002; Schanda and Brutscher 2005; Deschamps and Campbell 2006; Bermel et al. 2009b) and non-uniform sampling (NUS) (Malmodin and Billeter 2005; Hiller et al. 2005; Atreya and Szyperski 2005; Lescop et al. 2007; Jaravine et al. 2008; Kazimierczuk et al. 2010, 2012; Zawadzka-Kazimierczuk et al. 2012) of indirect evolution time space of multidimensional NMR experiments have been proposed to either reduce experimental time or improve spectral resolution; the joint use of these advancements has been reported (Bermel et al. 2009b; Bertini et al. 2011b; Novácek et al. 2011). Completely automated analysis of higher dimensionality spectra was shown to be very useful for the study of large IDPs (Narayanan et al. 2010).

Starting from the above results, we have developed a suite of ^{13}C detected multidimensional NMR experiments to exploit the best spin properties for a reliable and accurate sequence specific assignment. The determination of chemical shifts forms the basis for the structural and dynamic characterization of IDPs and of their interactions at atomic resolution. The proposed methodology can extend the size of IDPs that can be investigated by NMR. The new methods were demonstrated on a paradigmatic intrinsically disordered protein, human α-synuclein (14,460 Da).

Materials and methods

All NMR experiments were performed at 16.4 T on a Bruker Avance spectrometer operating at 700.06 MHz ^{1}H and 176.03 MHz ^{13}C frequencies, equipped with a cryogenically cooled probehead optimized for ^{13}C-direct detection. A sample of 1.2 mM uniformly ^{13}C, ^{15}N labeled human α-synuclein in 20 mM phosphate buffer at pH 6.5 was prepared as previously described (Huang et al. 2005). EDTA and NaCl were added to reach the final concentration of 0.5 and 200 mM, respectively, and 10 % D_2O was added for the lock. All experiments were acquired at 285.5 K. Parameters specific to each experiment are reported in the captions of the figures describing the pulse sequences, all reported in the Supplementary Material. For ^{13}C band-selective $\pi/2$ and π flip angle pulses Q5 (or time reversed Q5) and Q3 shapes (Emsley and Bodenhausen, 1992) of durations of 300 and 220 μs, respectively, were used, except for the π pulses that should be band-selective on the C^{α} region (Q3, 860 μs) and for the adiabatic π pulse to invert both C' and C^{α} [smoothed Chirp 500 μs, 25 % smoothing, 80 kHz sweep width, 11.3 kHz RF field strength (Boehlen and Bodenhausen 1993)]. The ^{13}C band selective pulses on C^{ali}, C^{α}, and C' were given at the center of each region, respectively, and the adiabatic pulse was adjusted to cover the entire ^{13}C region. Decoupling of ^{1}H and ^{15}N was achieved with waltz16 (Shaka et al. 1983) (1.7 kHz) and garp4 (Shaka et al. 1985) (1.0 kHz) sequences, respectively. All gradients employed had 1 ms of duration and a sine-shape. Each experiment was acquired in a pseudo 2D mode, with States method applied in all indirect dimensions to achieve quadrature detection. All experiments employ the IPAP approach (Bermel et al. 2008) to remove the splitting in the direct acquisition dimension caused by the C^{α}–C' couplings. The in-phase (IP) and antiphase (AP) components were acquired and stored in an interleaved manner, doubling the number of FIDs recorded. The spin-state-selection approach can also be implemented to achieve ^{15}N decoupling in order to be able to extend the acquisition time of the FID without limitations imposed by ^{15}N decoupling (Bermel et al. 2009a). The experimental parameters used for the acquisition of all experiments proposed here are reported in Table 1. All nD experiments ($n \geq 3$) were performed using on-grid non-uniform sampling. "Poisson disk" sampling scheme (Kazimierczuk et al. 2008) was chosen to generate the time schedules with *RSPack* software. All the spectra were acquired using *Bruker TopSpin 1.3* software. The experimental data were converted with *nmrPipe* and then processed using the Sparse Multidimensional Fourier Transform (SMFT) (Kazimierczuk et al. 2007) implemented in *ToASTD* (Kazimierczuk et al. 2006) and *reduced* (Kazimierczuk et al. 2009) (for 3D and 4D spectra,

Table 1 Experimental parameters used for the multidimensional NMR experiments

	Spectral widths and maximal evolution times				No. of scans	Inter-scan delay (s)	No. of complex points (aq)	No. of hypercomplex points	Duration of the experiment	Relative data points density (%)
4D	8,800 Hz	2,500 Hz (^{15}N)	12,500 Hz ($^{13}C^{\alpha,\beta}$)	5,000 Hz (^{1}H)	4	1.1	512	1,200	1 day, 4 h	0.053
HCBCACON	(^{13}C′)	30 ms	6 ms	10 ms						
3D	8,800 Hz	2,500 Hz (^{15}N)	12,500 Hz ($^{13}C^{\alpha,\beta}$)		4	1.1	512	600	7 h	2.67
(H)CBCACON	(^{13}C′)	30 ms	6 ms							
4D	8,800 Hz	3,500 Hz (^{15}N)	12,500 Hz ($^{13}C^{ali}$)	5,000 Hz (^{1}H)	4	1.1	512	1,800	1 day, 19 h	0.015
HCCCON	(^{13}C′)	28 ms	12 ms	20 ms						
3D	8,800 Hz	3,500 Hz (^{15}N)	12,500 Hz ($^{13}C^{ali}$)		4	1.1	512	600	7 h	1.00
(H)CCCON	(^{13}C′)	28 ms	12 ms							
4D	8,800 Hz	2,500 Hz (^{15}N)	12,500 Hz ($^{13}C^{\alpha,\beta}$)	5,000 Hz (^{1}H)	4	1.2	512	1,080	1 day, 5 h	0.024
HCBCANCO	(^{13}C′)	30 ms	7.2 ms	20 ms						
4D/5D[a]	8,800 Hz	2,500 Hz (^{15}N)	4,400 Hz ($^{13}C^{\alpha}$)	2,500 Hz (^{15}N)	8	0.5	1,024	720	23 h	0.010
(H^{N}-flip)NCANCO	(^{13}C′)	24 ms	45 ms	30 ms						
3D	8,800 Hz	2,500 Hz (^{15}N)		2,500 Hz (^{15}N)	8	0.5	1,024	960	18 h	5.33
(H^{N}-flip)NCANCO	(^{13}C′)	24 ms		30 ms						
4D/5D[b]	8,800 Hz	2,500 Hz (^{15}N)	4,400 Hz ($^{13}C^{\alpha}$)	2,500 Hz (^{15}N)	4	0.7	512	2,000	1 day, 12 h	0.036
(H^{N}-flip)NCACON	(^{13}C′)	40 ms	24 ms	24 ms						
3D	8,800 Hz	2,500 Hz (^{15}N)		2,500 Hz (^{15}N)	4	0.7	512	2,000	18 h	8.34
(H^{N}-flip)NCACON	(^{13}C′)	40 ms		24 ms						
3D	10,000 Hz	4,000 Hz (^{15}N)	6,250 Hz ($^{13}C^{\alpha}$)		8	1.2	512	480	12 h	0.65
(H)CANCACO	(^{13}C′)	30 ms	24.8 ms							

[a] This experiment was also run in the 5D mode including ^{1}H evolution (spectral width 2,000 Hz, maximal evolution time 20 ms, 480 hypercomplex points, 1 day and 6 h duration, relative data points density 0.000077 %, all the other parameters remaining the same)

[b] This experiment was also run in the 5D mode including ^{1}H evolution (spectral width 2,000 Hz, maximal evolution time 20 ms, 400 hypercomplex points, 15 h duration, relative data points density 0.000090 %, all the other parameters remaining the same)

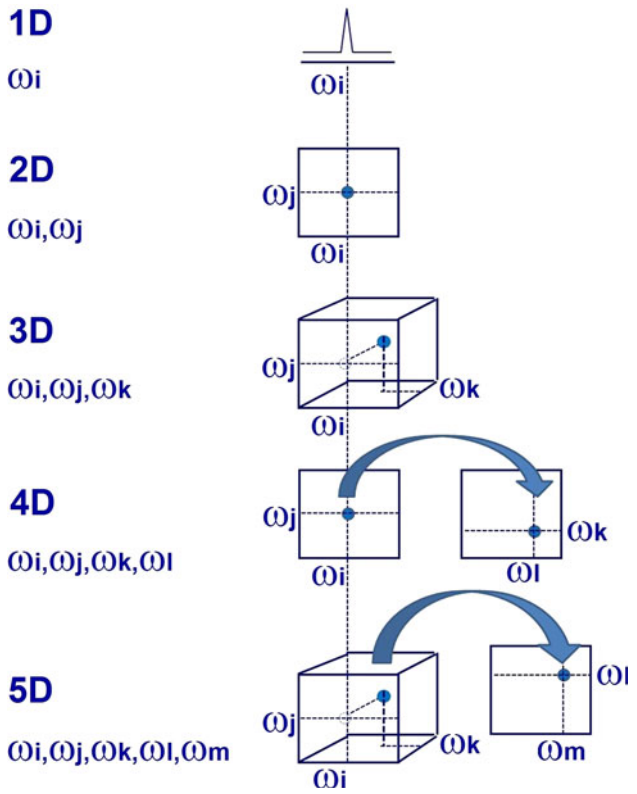

Fig. 1 The progressive walk towards experiments of higher dimensionality is schematically illustrated, together with an intuitive approach to easily visualize the information content of experiments with more than three dimensions

respectively), included in the *MFT* package software. For on-grid non-uniformly sampled 4D spectra, *cleaner4d* and *reconstructor4d* (Stanek et al. 2012) included in the SSA (Signal Separation Algorithm) software package, were used to suppress sampling artifacts. Finally, the programs *Sparky* (Goddard and Kneller 2000) and *Cara* (Keller 2004) were used for visualization of spectra and assignment of resonances. The *RSPack*, *ToASTD*, *reduced*, *cleaner*, and *reconstructor* software are available on-line (http://nmr700.chem.uw.edu.pl/).

Results and discussion

The use of high-dimensional NMR spectra (4D, 5D, etc.) for biomolecular NMR applications has not yet become routine despite its great potential. The improvement in resolution that can be obtained by addition of an extra dimension can easily be imagined when passing from 1D to 2D, then to 3D (Fig. 1). However, the analysis of NMR spectra of higher dimensionality than three might appear difficult. Surprisingly, the extension beyond 3D may be explained in a fairly simple way. For example, a 4D spectrum can be imagined by associating to each cross peak in a 2D spectrum two extra dimensions, as schematically indicated in Fig. 1. Since many different 4D spectra that can be designed correlate a common pair of spin resonances in two of the detected dimensions (a common 2D reference plane), these two dimensions can be taken as a common reference for the analysis of 4D spectra. The information about the other nuclear spins to which they are correlated in the different 4D variants can be achieved by inspection of the 2D planes associated to each of the cross peaks in the 2D map selected as a reference. Of course the same concepts can easily be extended to the analysis of a 5D, by choosing a 3D as a reference spectrum and then, for each of the cross peaks identified in the 3D, inspecting the related 2D spectrum (or, of course, vice versa). This easy way to visualize multidimensional NMR spectra, at the heart of the recently proposed way to process multidimensional NMR spectra (SMFT) (Kazimierczuk et al. 2007), represents a very good approach to retain simple intuition for the analysis of the data, still of course amenable to automation. From a more practical point of view, the SMFT approach allows also to maintain high digital and spectral resolution in all the detected dimensions without dramatic increase of file sizes, a key aspect to fully exploit the potential of multidimensional NMR experiments in particular for the study of IDPs.

In our experimental strategy, schematically illustrated in Fig. 2, the 2D CON was chosen as a reference spectrum (Bermel et al. 2006a), owing to its excellent resolution that can be obtained also in case of intrinsically disordered proteins (Fig. 3A). This experiment correlates two heteronuclei of neighboring aminoacids [the carbonyl carbon of one aminoacid residue (C_i') with the nitrogen of the following one (N_{i+1})]. In the first stage of the sequence specific assignment process, the identification of aminoacid type is based on the 4D HCBCACON and 4D HCCCON cross-sections (H^{ali}–C^{ali} planes) extracted for each CON cross peak. The H^{ali}–C^{ali} plane of the 4D HCBCACON and 4D HCCCON spectra show the one bond H^{α}–C^{α}/H^{β}–C^{β} correlations as well as all H^{ali}–C^{ali} correlations of the entire aminoacid side chain, respectively (Fig. 3B–E). The information content of the 2D H^{ali}–C^{ali} cross-sections of these 4D experiments appears quite similar to that of a ^{1}H–^{13}C 2D correlation spectrum; however, without the resolution provided by the CON, all the signals of aminoacids of the same type would cluster at very similar chemical shifts, preventing their identification and assignment. Instead, the inspection of the H^{ali}–C^{ali} planes at specific C_i'–N_{i+1} frequencies (specific cross peaks in the CON spectrum) enables us to classify the different CON cross peaks to different kinds of aminoacids (or aminoacid-groups) and of course to determine the H^{ali}–C^{ali} chemical shifts. It is worth noting that thanks to NUS and SMFT the

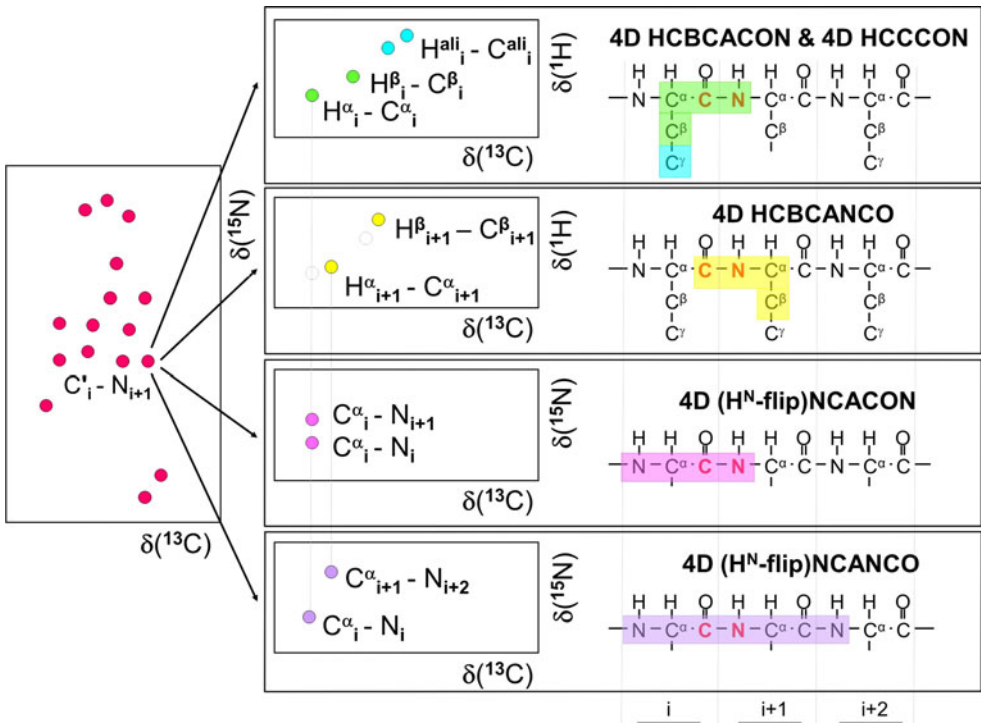

Fig. 2 A schematic illustration of the experimental strategy proposed. The 4D experiments share as common features the direct detection of ^{13}C, in particular of carbonyls (C_i'), as well as the evolution of the chemical shift of the attached ^{15}N (N_{i+1}) in one of the indirect dimensions. For this reason, the 2D CON is chosen as a common reference, as indicated schematically on the *left hand side*. The information content of the various 4D experiments can then be simplified considering that for each cross peak in the 2D CON (C_i'–N_{i+1}) one can extract the associated 2D plane, which provides a specific information depending on the design of the particular 4D. The correlations expected in the two additional dimensions for each of the 4Ds are schematically illustrated. For clarity, the nuclei involved in the coherence transfer pathways are also *highlighted* on the backbone of the protein

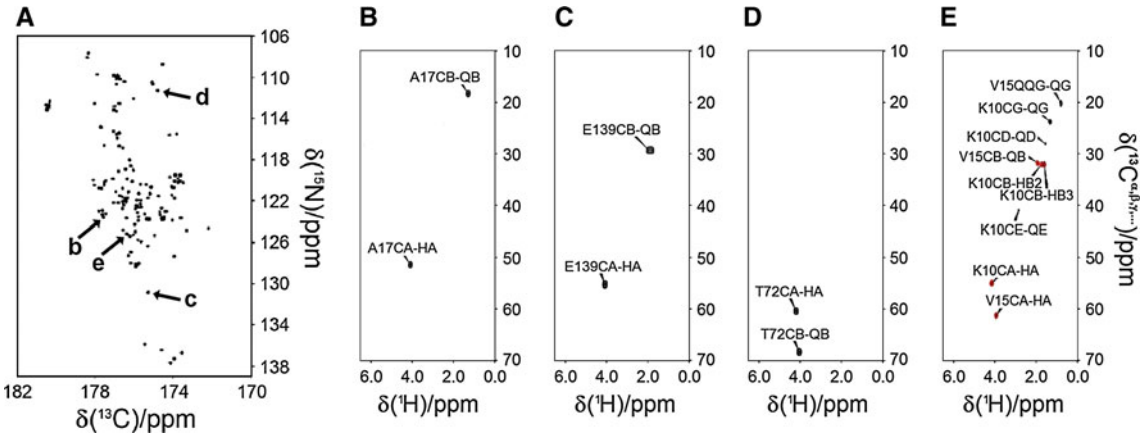

Fig. 3 The information content of the 4D HCBCACON and 4D HCCCON is illustrated. Panel **A** reports the reference 2D CON spectrum. The ^{1}H–^{13}C planes extracted from the 4D HCBCACON at the frequencies corresponding to cross peaks indicated in the CON spectrum (Panel **A**) as *b*, *c* and *d* are shown in panels **B**, **C** and **D** respectively. The ^{1}H–^{13}C planes extracted from the 4D HCBCACON and 4D HCCCON at the frequencies corresponding to the cross peak indicated as *e* are overlaid in panel **D**

excellent resolution in all dimensions of these experiments was obtained in about 1 day.

The next step is aimed at collecting information for unambiguous sequence specific assignment. In general, the most commonly employed strategy for sequence specific assignment exploits the N–C^{α} scalar couplings that enable us to correlate the C^{α} (and the attached C^{β}) of one aminoacid (C_i^{α}) to its own nitrogen (N_i) and to the one of the following aminoacid (N_{i+1}). The experiment providing this information in the suite of exclusively heteronuclear NMR

experiments based on ^{13}C direct detection (Felli and Pierattelli 2012) is the 3D (H)CBCANCO (Bermel et al. 2009a). This can be easily extended to 4D by implementing ^{1}H evolution in the additional indirect dimension. Therefore for each CON cross peak (C_i', N_{i+1}) the 4D HCBCANCO can be inspected to identify the H^{α}–C^{α} and H^{β}–C^{β} correlations of the following aminoacid as schematically shown in Fig. 2. This method performs well as long as aminoacids with significantly different H^{α}–C^{α} and H^{β}–C^{β} chemical shifts are next to each other in the primary sequence of the protein. However, it may leave some ambiguities if neighboring aminoacids feature similar H^{β}–C^{β} chemical shifts, a condition that often occurs in IDPs. Backbone nuclear spins, which are more heavily influenced by the contributions of the preceding and following aminoacids, retain larger chemical shift dispersion also in IDPs. Therefore, they are well suited to provide sufficient information to resolve ambiguities in linking the identified aminoacid spin systems in a sequence specific manner. As

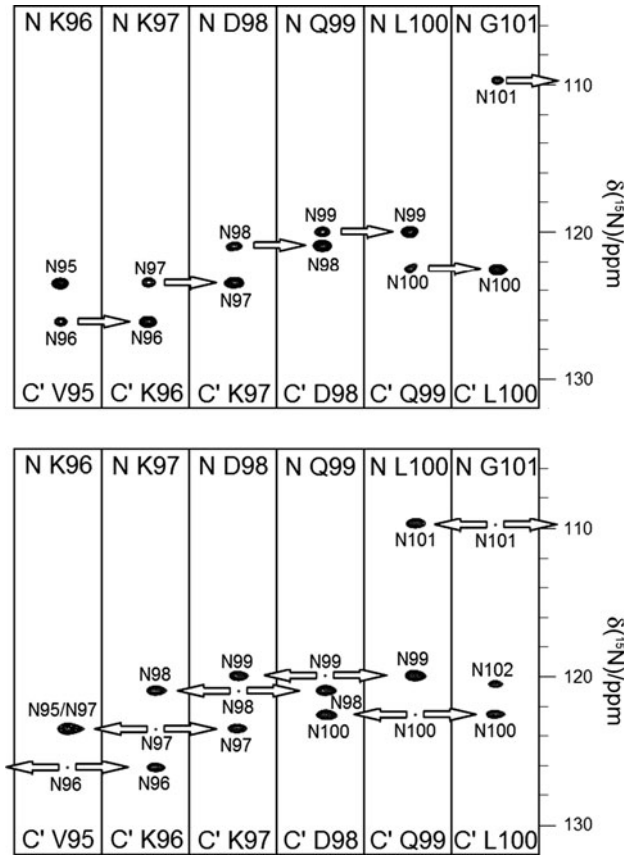

Fig. 4 The strip plots extracted from the (H^N-flip)N(CA)CON (*top*) and (H^N-flip)N(CA)NCO (*bottom*) experiments acquired in the 3D mode evolving ^{15}N chemical shifts in the indirect dimensions are shown for aminoacids 95–101 of human α-synuclein. The labels on the bottom of each strip indicate the C_i' resonance frequencies while those on top the N_{i+1} resonance frequency at which strips were extracted. The dots in the strips of the second panel indicate the C_i'–N_{i+1}–N_{i+1} frequencies

the chemical shift dispersion increases from ^{1}H via ^{13}C to ^{15}N, the most promising heteronuclei to be exploited are backbone nitrogen nuclei. Additionally, the efficient chemical exchange processes of amide protons, typical for solvent exposed backbone sites in IDPs, enables us to take advantage of the faster selective longitudinal relaxation properties of amide protons by implementing the H^N-flip approach (Bermel et al. 2009b; Bertini et al. 2011b). The latter allows us to reduce significantly the inter-scan delay and, as a consequence, the overall duration of NMR experiments. The selective manipulation of amide protons through the H^N-flip approach, while restoring the H_2O resonance to the equilibrium condition, also improves the sensitivity of the experiment as losses due to exchange processes are minimal. The H^N-flip approach was thus implemented in two multidimensional ^{13}C detected NMR experiments, namely the HNCACON and HNCANCO which are hereafter referred to as (H^N-flip)NCACON and (H^N-flip)NCANCO. The coherence transfer pathway as well as the scheme of correlations expected in the spectra are shown in Fig. 2.

To show the efficiency of the approach, the strips corresponding to the 95–101 fragment of human α-synuclein were extracted from the 3D (H^N-flip)N(CA)CON and the 3D (H^N-flip)N(CA)NCO, in which nitrogen spins are evolved in indirect dimensions (Fig. 4). This clearly highlights the complementary information provided by these experiments which enables one to achieve robust information to eliminate ambiguities in the sequence specific assignment. Indeed, in case of the 3D (H^N-flip)N(CA)CON each C_i'–N_{i+1} cross peak is correlated to the nitrogen of residue i (N_i), while in the 3D (H^N-flip)N(CA)NCO the coherence transfer pathway is optimized for the detection of the correlation to the nitrogen of residue i (N_i) and i + 2 (N_{i+2}). To further reduce the ambiguities and confirm the information obtained the 4D versions of such experiments can be acquired, in which the C^{α} chemical shifts are also evolved in an additional indirect dimension. Again, for each cross peak present in the reference 2D CON spectrum, the corresponding 2D N/C^{α} plane shows additional correlations to perform sequence specific assignment. As an example, Fig. 5 shows the 2D N/C^{α} planes extracted from the 4D (H^N-flip)NCACON for residues 8–12 of human α-synuclein. It is worth noting that the extension to 4D enables us to resolve, in the second plane shown (for S9/K10), three different sets of correlations that would have been difficult to disentangle otherwise. The (H^N-flip)NCANCO allows also to link C_i',N_{i+1} to the i + 2 residue, as shown in Fig. 6 for the fragment 69–72 of human α-synuclein. Therefore, the 4D (H^N-flip)NCACON and 4D (H^N-flip)NCANCO experiments provide an excellent tool to resolve ambiguities in the sequence specific assignment process thanks to a wealth of

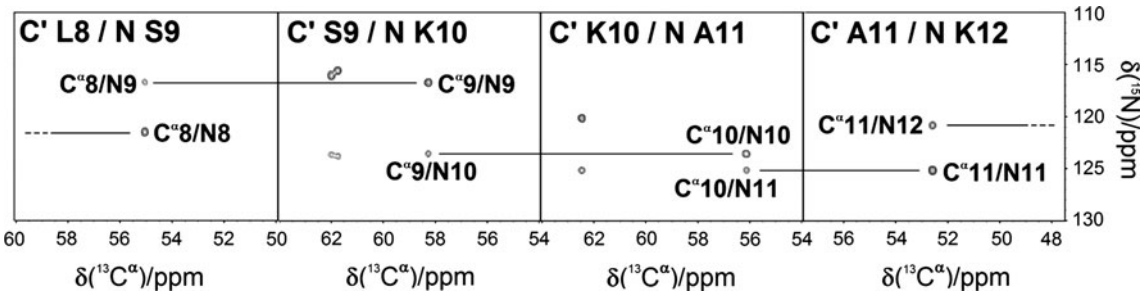

Fig. 5 As an example of the information content of the 4D (H^N-flip)NCACON experiment, the figure shows the 2D N/C^α (F_1/F_2) planes of the full 4D spectrum, extracted for 4 peaks of the 2D CON reference plane (C_i' and N_{i+1} frequencies are indicated in the *top left* of each cross-section corresponding to aminoacids 8–12 of human α-synuclein). The sequential assignment of spin systems, which of course follows the same strategy described for 3D version, becomes more robust thanks to the improved resolution provided by the additional C^α dimension (inspecting 2D planes rather than 1D strips simplifies the analysis as potential ambiguities are clearly resolved). As an example, in the second and third 2D N/C^α planes displayed from the left, it is possible to distinguish 3 and 2 spin systems respectively, which are not resolved in the corresponding strips extracted from the 3D version of the experiment

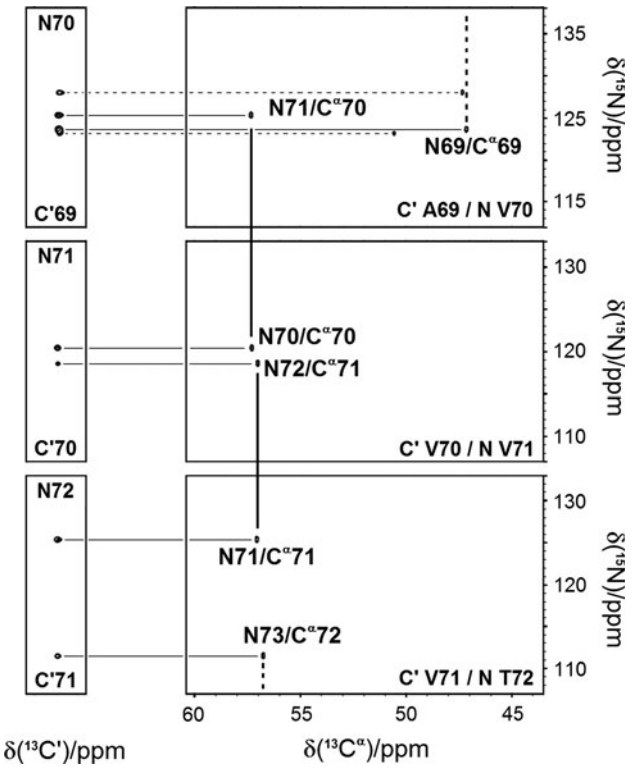

Fig. 6 The 2D N/C^α planes of the full 4D (H^N-flip)NCANCO spectrum for three cross peaks in the reference 2D CON plane as indicated in the *bottom right* of each plane (C_i'–N_{i+1} frequencies). For clarity, also the strips extracted for the same cross peaks in the reference 2D CON plane from the 3D (H^N–flip)N(CA)NCO spectrum are shown on the left. In such 2D N/C^α cross-sections of the full 4D spectrum, correlations observed were N_i–C_i^α and N_{i+2}–C_{i+1}^α. Thus, sequential assignment was established along the $^{13}C^\alpha$ dimension, while the ^{15}N dimension was exploited for better cross-peak dispersion. In particular, in the cross-section shown on the top it is possible to distinguish peaks belonging to 2 different spin systems, which are not resolved in the corresponding strips of the analogous 3D experiment

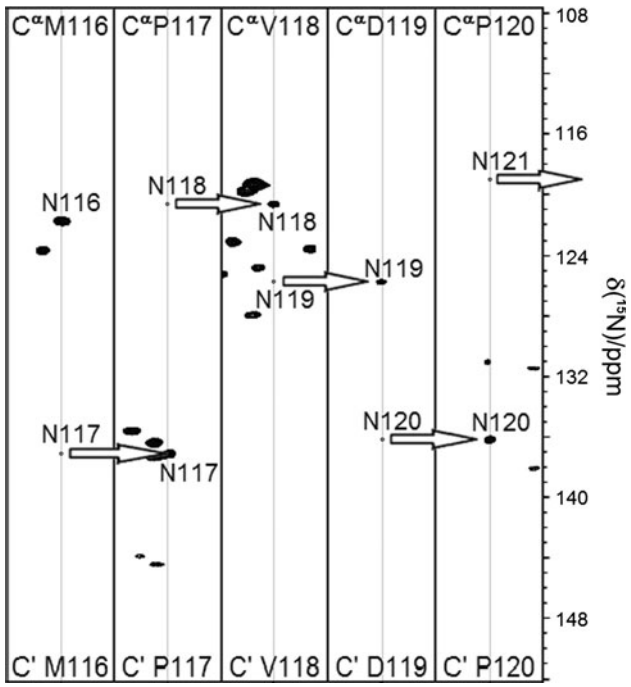

Fig. 7 The strips extracted from the 3D (HCA)NCACO experiment at C_i'–C_i^α frequencies (of residues indicated at the *top* of each strip) with ^{15}N in the indirect dimension are shown for aminoacids 116–120 of human α-synuclein. The frequencies of the C_i'–C_i^α–N_{i+1} cross-peaks (shown as *dots* in the figure) can be taken from the (H)CBCACON

(complementary) correlations that can be detected. The performance of these two experiments largely benefits from the efficient exchange of amide protons, which contributes to the longitudinal relaxation enhancement (LRE) of amide protons exploited through the H^N-flip approach (Bermel et al. 2009b; Bertini et al. 2011b). However, in cases in which amide proton resonances are broadened beyond detection or for proline residues, which are quite abundant in IDPs and lack an amide proton, the two

experiments described above do not provide information. Therefore, an additional experiment, the (HCA)NCACO, that exploits the H^{α}, instead of the H^{N}, as a starting source of polarization was designed to provide complementary information. A few strips extracted from this spectrum (acquired in the 3D mode) provide the desired information necessary for the sequence specific assignment as shown for the fragment 116–120 of human α-synuclein (Fig. 7). The H^{α}-flip approach (Bermel et al. 2009b; Bertini et al. 2011a) can be also easily implemented to enhance longitudinal relaxation in the (HCA)NCACO experiment. However, in case of highly flexible polypeptides such as it often occurs when dealing with IDPs, this is generally less efficient.

The latter three experiments described, which exploit correlations involving backbone heteronuclei for sequence specific assignment, were acquired evolving *heteronuclear* chemical shifts *only*. If necessary, an additional dimension to include proton evolution, which is already used as a starting polarization source, can be introduced to further increase the resolution and to achieve also proton signal assignment. The 5D HNCACON/5D HNCANCO and 4D HCANCACO experiments were acquired and the respective pulse sequences are available in the Supplementary Material (Figure S6).

To conclude, the ^{13}C direct detection suite of multidimensional NMR experiments proposed here (*nD-CON-based suite*) can be acquired in a short time preserving excellent spectral resolution in 3D, 4D and, if necessary, also in 5D versions, thanks to non-uniform sampling, H-excitation and H^{N}-flip approaches and SMFT processing of the data. This set of ^{13}C detected NMR experiments provides a stand-alone tool to investigate IDPs or IDRs of increasing size and complexity.

Supplementary material

4D HCBCACON, 4D HCCCON, 4D HCBCANCO, 4/5D (H^{N}-flip)NCANCO, 4/5D (H^{N}-flip)NCACON, 3/4D (HCA)NCACO pulse sequences; experimental parameters for the recorded experiments.

Acknowledgments This work has been supported in part by the EC 7th Framework program BioNMR, contract 261863 and by the EC Marie Curie ITN program (IDPbyNMR, contract 264257).

References

Atreya HS, Szyperski T (2005) Rapid NMR data collection. Methods Enzymol 394:78–108

Bermel W, Bertini I, Felli IC, Kümmerle R, Pierattelli R (2003) ^{13}C direct detection experiments on the paramagnetic oxidized monomeric copper, zinc superoxide dismutase. J Am Chem Soc 125:16423–16429

Bermel W, Bertini I, Felli IC, Kümmerle R, Pierattelli R (2006a) Novel ^{13}C direct detection experiments, including extension to the third dimension, to perform the complete assignment of proteins. J Magn Reson 178:56–64

Bermel W, Bertini I, Felli IC, Lee Y-M, Luchinat C, Pierattelli R (2006b) Protonless NMR experiments for sequence-specific assignment of backbone nuclei in unfolded proteins. J Am Chem Soc 128:3918–3919

Bermel W, Bertini I, Felli IC, Piccioli M, Pierattelli R (2006c) ^{13}C-detected *protonless* NMR spectroscopy of proteins in solution. Progr NMR Spectrosc 48:25–45

Bermel W, Felli IC, Kümmerle R, Pierattelli R (2008) ^{13}C direct-detection biomolecular NMR. Concepts Magn Reson 32A:183–200

Bermel W, Bertini I, Csizmok V, Felli IC, Pierattelli R, Tompa P (2009a) H-start for exclusively heteronuclear NMR spectroscopy: the case of intrinsically disordered proteins. J Magn Reson 198:275–281

Bermel W, Bertini I, Felli IC, Pierattelli R (2009b) Speeding up ^{13}C direct detection NMR experiments. J Am Chem Soc 131:15339–15345

Bermel W, Bertini I, Felli IC, Peruzzini R, Pierattelli R (2010) Exclusively heteronuclear NMR experiments to obtain structural and dynamic information on proteins. ChemPhysChem 11:689–695

Bertini I, Felli IC, Gonnelli L, Vasantha Kumar MV, Pierattelli R (2011a) ^{13}C direct-detection biomolecular NMR spectroscopy in living cells. Angew Chem Int Ed 50:1–4

Bertini I, Felli IC, Gonnelli L, Vasantha Kumar MV, Pierattelli R (2011b) High-resolution characterization of intrinsic disorder in proteins. ChemBioChem 12:2347–2352

Boehlen J-M, Bodenhausen G (1993) Experimental aspects of chirp NMR spectroscopy. J Magn Reson, Ser A 102:293–301

Csizmok V, Felli IC, Tompa P, Banci L, Bertini I (2008) Structural and dynamic characterization of intrinsically disordered human securing by NMR. J Am Chem Soc 130:16873–16879

Deschamps M, Campbell ID (2006) Cooling overall spin temperature: protein NMR experiments optimized for longitudinal relaxation effects. J Magn Reson 178:206–211

Dunker AK, Lawson JD, Brown CJ, Williams RM, Romero P, Oh JS, Ratliff CM, Hipps KW, Ausio J, Nissen MS, Reeves R, Kang C, Kissinger CR, Bailey RW, Griswold MD, Chiu W, Garner EC (2001) Intrinsically disordered protein. J Mol Graph Model 19:26–59

Dyson HJ, Wright PE (2004) Unfolded proteins and protein folding studied by NMR. Chem Rev 104:3607–3622

Dyson HJ, Wright PE (2005) Intrinsically unstructured proteins and their functions. Nat Rev Mol Cell Biol 6:197–208

Eliezer D (2009) Biophysical characterization of intrinsically disordered proteins. Curr Opin Struct Biol 19:23–30

Emsley L, Bodenhausen G (1992) Optimization of shaped selective pulses for NMR using a quaternion description of their overall propagators. J Magn Reson 97:135–148

Felli IC, Pierattelli R (2012) ^{13}C direct detection NMR. In: McGreevy KS, Parigi G (eds) Bertini I, NMR of biomolecules. Wiley-Blackwell, London, pp 433–442

Goddard TD, Kneller DG (2000) SPARKY 3. University of Califofnia, San Francisco

Hiller S, Fiorito F, Wüthrich K, Wider G (2005) Automated projection spectroscopy (APSY). Proc Natl Acad Sci USA 102:10876–10881

Hsu ST, Bertoncini CW, Dobson CM (2009) Use of protonless NMR spectroscopy to alleviate the loss of information resulting from exchange-broadening. J Am Chem Soc 131:7222–7223

Hu K, Vögeli B, Clore GM (2007) Spin-state selective carbon-detected HNCO with TROSY optimization in all dimensions and double echo-antiecho sensitivity enhancement in both indirect dimensions. J Am Chem Soc 129:5484–5491

Huang C, Ren G, Zhou H, Wang C (2005) A new method for purification of recombinant human alpha-synuclein in Escherichia coli. Protein Expr Purif 42:173–177

Jaravine VA, Zhuravleva AV, Permi P, Ibraghimov I, Orekhov VY (2008) Hyperdimensional NMR spectroscopy with nonlinear sampling. J Am Chem Soc 130:3927–3936

Kazimierczuk K, Zawadzka A, Koźmiński W, Zhukov I (2006) Random sampling of evolution time space and Fourier transform processing. J Biomol NMR 36:157–168

Kazimierczuk K, Zawadzka A, Koźmiński W, Zhukov I (2007) Lineshapes and artifacts in multidimensional Fourier transform of arbitrary sampled NMR data sets. J Magn Reson 188:344–356

Kazimierczuk K, Zawadzka A, Koźmiński W (2008) Optimization of random time domain sampling in multidimensional NMR. J Magn Reson 192:123–130

Kazimierczuk K, Zawadzka A, Koźmiński W (2009) Narrow peaks and high dimensionalities: exploiting the advantages of random sampling. J Magn Reson 197:219–228

Kazimierczuk K, Stanek J, Zawadzka-Kazimierczuk A, Koźmiński W (2010) Random sampling in multidimensional NMR spectroscopy. Prog NMR Spectrosc 57:420–434

Kazimierczuk K, Misiak M, Stanek J, Zawadzka-Kazimierczuk A, Koźmiński W (2012) Generalized Fourier transform for non-uniform sampled data. Top Curr Chem 316:79–124

Keller RLJ (2004) The computer aided resonance assignment tutorial. Cantina Verag, Goldau

Kjaergaard M, Poulsen FM (2011) Sequence correction of random coil chemical shifts: correlation between neighbor correction factors and changes in the Ramachandran distribution. J Biomol NMR 50:157–165

Kjaergaard M, Brander S, Poulsen FM (2011) Random coil chemical shift for intrinsically disordered proteins: effects of temperature and pH. J Biomol NMR 49:139–149

Knoblich K, Whittaker S, Ludwig C, Michiels P, Jiang T, Schaffhausen B, Günther U (2009) Backbone assignment of the N-terminal polyomavirus large T antigen. Biomol NMR Assign 3:119–123

Lescop E, Schanda P, Brutscher B (2007) A set of BEST triple resonance experiments for time-optimized protein resonance assignment. J Magn Reson 187:163–169

Malmodin D, Billeter M (2005) Multiway decomposition of NMR Spectra with coupled evolution periods. J Am Chem Soc 127:13486–13487

Mittag T, Forman-Kay J (2007) Atomic-level characterization of disordered protein ensembles. Curr Opin Struct Biol 17:3–14

Narayanan RL, Duerr HN, Bilbow S, Biernat J, Mendelkow E, Zweckstetter M (2010) Automatic assignment of the intrinsically disordered protein Tau with 441-residues. J Am Chem Soc 132:11906–11907

Nováček J, Zawadzka-Kazimierczuk A, Papoušková V, Žídek L, Šanderová H, Krásny L, Koźmiński W, Sklenář V (2011) 5D ^{13}C-detected experiments for backbone assignment of unstructured proteins with a very low signal dispersion. J Biomol NMR 50:1–11

O'Hare B, Benesi AJ, Showalter SA (2009) Incorporating ^{1}H chemical shift determination into 13C-direct detected spectroscopy of intrinsically disordered proteins in solution. J Magn Reson 200:354–358

Pasat G, Zintsmaster JS, Peng J (2008) Direct ^{13}C-detection for carbonyl relaxation studies of protein dynamics. J Magn Reson 193:226–232

Pérez Y, Gairi M, Pons M, Bernadò P (2009) Structural characterization of the natively unfolded N-terminal domain of human c-Src kinase: insights into the role of phosphorylation of the unique domain. J Mol Biol 391:136–148

Pervushin K, Vogeli B, Eletsky A (2002) Longitudinal ^{1}H relaxation optimization in TROSY NMR spectroscopy. J Am Chem Soc 124:12898–12902

Schanda P, Brutscher B (2005) Very fast two-dimensional NMR spectroscopy for real-time investigation of dynamic events in proteins on the time scale of seconds. J Am Chem Soc 127:8014–8015

Schanda P, Van Melckebeke H, Brutscher B (2006) Speeding up three-dimensional protein NMR experiments to a few minutes. J Am Chem Soc 128:9042–9043

Serber Z, Richter C, Moskau D, Boehlen J-M, Gerfin T, Marek D, Haeberli M, Baselgia L, Laukien F, Stern AS, Hoch JC, Dötsch V (2000) New carbon-detected protein NMR experiments using cryoprobes. J Am Chem Soc 122:3554–3555

Shaka AJ, Keeler J, Freeman R (1983) Evaluation of a new broadband decoupling sequence: WALTZ-16. J Magn Reson 53:313–340

Shaka AJ, Barker PB, Freeman R (1985) Computer-optimized decoupling scheme for wideband applications and low-level operation. J Magn Reson 64:547–552

Shimba N, Kovacs H, Stern AS, Nomura AM, Shimada I, Hoch JC, Craik CS, Dötsch V (2005) Optimization of ^{13}C direct detection NMR methods. J Biomol NMR 30:175–179

Stanek J, Augustyniak R, Koźmiński W (2012) Suppression of sampling artefacts in high-resolution four-dimensional NMR spectra using signal separation algorithm. J Magn Reson 214:91–102

Tompa P (2002) Intrinsically unstructured proteins. Trends Biochem Sci 27:527–533

Tompa P (2009) Structure and function of intrinsically disordered proteins. Taylor and Francis Group, Boca Raton

Uversky VN, Gillespie JR, Fink AL (2000) Why are "natively unfolded" proteins unstructured under physiologic conditions? Proteins Struct Funct Genet 41:415–427

Wright PE, Dyson HJ (1999) Intrinsically unstructured proteins: re-assessing the protein structure-function paradigm. J Mol Biol 293:321–331

Zawadzka-Kazimierczuk A, Koźmiński W, Šanderová H, Krásny L (2012) High dimensional and high resolution pulse sequences for backbone resonance assignment of intrinsically disordered proteins. J Biomol NMR 52:329–337

Zhang H, Neal S, Wishart DS (2003) RefDB: a database of uniformly referenced protein chemical shifts. J Biomol NMR 25:173–195